


Dual Shapiro steps and fundamental transconductance in dc driven Bloch transistor

A. B. Zorin 

We propose a superconducting circuit based on the Bloch transistor, a quantum device consisting of two small-capacitance Josephson junctions connected in series and having a small island in between. This device is driven by two dc electrical sources controlling Josephson oscillations of frequency $f_J = 2e\overline{V}_J/h$, related to the average voltage \overline{V}_J on the transistor, and Bloch oscillations of frequency $f_B = \overline{I}_B/2e$, related to the average current \overline{I}_B injected into the transistor island. Due to the Bloch transistor properties, these two types of oscillations can mutually phase lock, i.e., $f_J = f_B$. This leads to formation of current steps on the current-voltage curve at $\overline{I}_B = 2ef_J$, which are similar to the dual Shapiro steps appearing at current $\overline{I} = 2ef$ under microwave irradiation of frequency f . Moreover, transconductance $\overline{I}_B/\overline{V}_J$ takes the fundamental value of $1/R_Q$, where $R_Q = h/4e^2$ is the resistance quantum. The obtained results pave the way to the alternative quantum standard of resistance, based on the superconducting circuit and operating without applying strong magnetic field.

I. INTRODUCTION

Significant progress in manufacturing small superconducting tunnel junctions made it possible the rapid growth of solid-state quantum technologies including development of Josephson qubits [1–4]. These circuits exploit multi-band structure of energy spectrum enabling quantum engineering of two-level systems [5] with high fidelity [6]. The development of superconducting quantum circuits exploiting the properties of the ground state was not, however, so rapid. As was predicted in 1985 [7, 8], these circuits, being fed by constant current I , generate Bloch oscillations with frequency $f_B = I/2e$. This phenomenon is associated with tunneling of single Cooper pairs and it is dual to ac Josephson effect [9]. Similar to Shapiro steps appearing on the I-V curves of microwave-irradiated Josephson junctions, the ac driven Bloch circuits demonstrate on their I-V curves the so-called dual Shapiro steps at $I = 2nef$, where f is the frequency of external ac signal and n is an integer. Slowdown of the experiments with Bloch oscillations can be explained by serious problems in implementation of compact high-ohmic impedance in biasing circuits, $|Z| \gg R_Q = h/4e^2 \approx 6.453 \text{ k}\Omega$, where R_Q is the resistance quantum [10–14]. Such high impedance is necessary for efficient suppression of quantum fluctuations of charge in the frequency range up to tens of GHz [7, 8].

Significant improvement of the Bloch circuits has been made using high-quality ultra-high-ohmic microstripline resistors [15] and the so-called superinductors. The latter elements are based on large kinetic inductance of either arrays of Josephson junctions [4] or superconducting granular microstrips [16]. Large superinductor in combination with serial resistance can substantially mitigate the problem of high-impedance implementation. Recently, several demonstrations of dual Shapiro steps using the superinductance concept have been reported by PTB-Braunschweig [17, 18], CNRS-Grenoble [19] and RHUL [20] groups. Similar dual Shapiro steps were also demonstrated in the experiment with microwave-driven quantum phase slip (QPS) circuits [21, 22]. Although the shape of the observed steps was not perfect, pre-

sumably because of considerable noise associated with high effective electron temperature and/or intensive microwave irradiation, the positions of the step centers were unambiguously related to the expected values of $I = 2nef$. Motivated by the results of these remarkable experiments, we propose an alternative Bloch-Josephson circuit enabling efficient phase lock of Bloch oscillations and, hence, observation of dual Shapiro steps without applying external microwave signal.

Our concept is based on the quantum properties of the Bloch transistor (BT), a three-terminal device made of two small serial Josephson junctions and a small superconducting island in between having a control gate electrode. The BT ground state is described by phase ϕ across the device and quasicharge q associated with the island [23–25]. Two electrical dc sources govern the dynamics of these variables; in particular, they control the frequencies of Josephson (f_J) and Bloch (f_B) oscillations, respectively. When these frequencies are close to each other, phase locking occurs, $f_J = f_B \equiv f$, and a step, similar to the dual Shapiro step under microwave irradiation, appears on I-V curve of dc driven BT at $I = 2ef_J$. Moreover, because f_J and f_B are related to voltage and current via the fundamental constants, $\Phi_0 = h/2e$ and $2e$, respectively, their phase locking results in quantization of the transconductance in units of R_Q^{-1} . Quantization of transconductance has been earlier found in a two-dimensional electron gas (2DEG), realized in a silicon field effect transistor in strong magnetic field [26] and this discovery had made great impact on quantum metrology [27]. Transconductance quantization was later predicted in multi-terminal Josephson circuits [28, 29], but to our best knowledge was not realized in experiment yet.

The idea of phase locking of the Bloch and Josephson oscillations was proposed by Likharev in 1986 [23]. It has been somewhat elaborated in Ref. [24], although without deep analysis and details of possible experiment. To the best of our knowledge, this idea was not experimentally realized, what was seemingly related to insufficiencies in fabrication technology and imperfections of low-noise cryogenic experiment at that time.

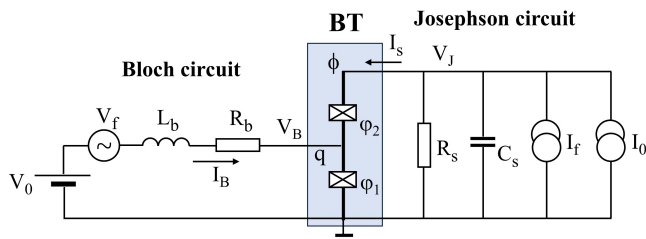


FIG. 1. Schematic of the proposed circuit including Bloch transistor (BT), outlined by grey rectangle, and the two complementary circuits, i.e., the Bloch and the Josephson circuits. The series Bloch circuit includes high-ohmic resistance R_b , inductance L_b , voltage noise source V_f , and constant voltage source V_0 . Current $I_B = dq/dt$ is injected into the BT island; the island voltage V_B depends on both quasicharge q and total phase ϕ . The parallel Josephson circuit comprises low-ohmic resistance R_s , rather large capacitance C_s , current noise source I_f , and constant current source I_0 . The BT voltage $V_J = d\phi/dt$, while supercurrent I_s depends on both phase ϕ and quasicharge q .

Finally we note, that an alternative approach to synchronization of the Bloch and Josephson oscillators has been proposed for a QPS circuit in Ref. [30]. The authors suggested a nanowire-based QPS element coupled to a *stand-alone* Josephson oscillator by means of a low-Q resonator. Recently, an attempt of integrating *individual* Josephson and Bloch oscillators on one chip was reported in Ref. [31]. In contrast to these circuits, the proposed circuit has neither a resonator (obviously shrinking a phase-locking range), nor an individual Josephson oscillator as such.

II. ELECTRICAL CIRCUIT

The schematic of our circuit is shown in Fig. 1. It consists of three parts: the Bloch circuit driven by constant voltage source V_0 , the Josephson circuit, driven by constant current source I_0 , and the BT enabling their coupling. Due to sufficiently low temperature and presumably slow dynamics, BT remains in the ground state. The parameters of the circuits are chosen such, that the two basic variables of the transistor, quasicharge q and overall phase $\phi = \varphi_1 + \varphi_2$ [23, 24], where $\varphi_{1,2}$ are individual phase drops on the junctions, are essentially decoupled from the environment and their behavior is classical. The dynamics of these variables is governed by voltage V_0 and current I_0 .

Resistance R_b , inserted in the Bloch circuit, is assumed to be sufficiently large [7, 8], so the corresponding dimensionless parameter is small,

$$\alpha_B = R_Q/R_b \ll 1. \quad (1)$$

Resistance R_b is compact, so its stray capacitance is small [15, 18]. Optional series (super)inductance L_b , like in re-

cent experiments of the RHUL group [20, 22], can notably improve decoupling of the BT island from the environment at high frequencies.

The Josephson part of the circuit includes the low-ohmic parallel resistance R_s , so the corresponding small dimensionless parameter is

$$\alpha_J = R_s/R_Q \ll 1. \quad (2)$$

The parallel capacitance C_s includes stray capacitances of resistor R_s and the wires connecting BT to current source I_0 . The shunting resistance R_s is responsible for unwanted fluctuations of phase ϕ (see, for example, Chapters 3 and 4 in Ref. [32]), so the value of R_s should be as low as possible. The physical dimensions of this resistance are practically limited by the size of the chip packaging, while the value of unavoidable capacitance C_s is not critical. So, we will assume that α_J is very small,

$$\alpha_J \ll \alpha_B \ll 1. \quad (3)$$

For typical experimental parameters of BT, having effective critical current I_c^* on the order of 10-100 nA [18, 20], and, say, resistance $R_s \sim 1 \Omega$, even huge capacitance $C_s \sim 1$ nF gives small value of the effective McCumber parameter [33, 34], $\beta_c = (2\pi/\Phi_0)I_c^*R_s^2C_s \lesssim 1$. Thus, the effective Josephson junction (in fact, the BT) is overdamped and the effect of capacitance C_s on its dynamics is indeed small [32].

Applying Kirchhoff's circuit laws, we obtain a set of two coupled equations, for the Bloch and Josephson circuits, respectively,

$$L_b \frac{d^2 q}{dt^2} + R_b \frac{dq}{dt} + V_B(q, \phi) = V_0 + V_f, \quad (4)$$

$$\frac{\Phi_0}{2\pi} C_s \frac{d^2 \phi}{dt^2} + \frac{\Phi_0}{2\pi} R_s^{-1} \frac{d\phi}{dt} + I_s(q, \phi) = I_0 + I_f. \quad (5)$$

Here we used the fact that gate current I_B and the Josephson voltage V_J (see Fig.1) are related to time derivatives of corresponding variables [7, 9],

$$I_B = dq/dt \quad \text{and} \quad V_J = (\Phi_0/2\pi)d\phi/dt. \quad (6)$$

Gate voltage V_B and Josephson supercurrent I_s depend on both variables, q and ϕ , and, hence, are responsible for their coupling. The shape of these double-periodic functions is determined by the BT parameters. The corresponding formulas will be derived in Sec. III B.

The last terms on the right hand sides of Eqs.(4) and (5), variables V_f and I_f , describe fluctuations in the Bloch and Josephson circuits, respectively. In the general case, their spectral densities are related to the real parts of the corresponding impedance and admittance [7, 8],

$$S_V(\omega) = \frac{R_b}{\pi} \frac{\hbar\omega}{2} \coth \frac{\hbar\omega}{2k_B T}, \quad (7)$$

$$S_I(\omega) = \frac{1}{\pi R_s} \frac{\hbar\omega}{2} \coth \frac{\hbar\omega}{2k_B T}. \quad (8)$$

In order to keep our analysis simple, the telegraph noise, associated with random appearance and disappearance of quasiparticles on the island [35], i.e., poisoning of the island, is not included in our model. So, we assume that in experiment, the chip includes, for example, appropriate quasiparticle traps [36] or has metallization of its back side [37], so the island is free of non-equilibrium quasiparticles.

III. BLOCH TRANSISTOR

The analysis of this remarkable device has been earlier reported, for example, in the papers about the BT-based electrometers [25, 38] and the charge-phase qubits [39–41]. Briefly, the Josephson junction free energies are [42]

$$\mathcal{E}_{1,2}(\varphi_{1,2}) = E_{J1,J2}(1 - \cos \varphi_{1,2}). \quad (9)$$

We admit that the Josephson energies, $E_{J1,J2} = (\Phi_0/2\pi)I_{c1,c2}$, and, hence, critical currents $I_{c1,c2}$, can be unequal. The sum of the two junction energies can be presented as [25]

$$\mathcal{E}_1 + \mathcal{E}_2 = -E_J(\phi) \cos[\varphi + \gamma(\phi)] + (E_{J1} + E_{J2}), \quad (10)$$

where the last term is an unimportant constant, while

$$E_J(\phi) = (E_{J1}^2 + E_{J2}^2 + 2E_{J1}E_{J2} \cos \phi)^{1/2}, \quad (11)$$

$$\phi = \varphi_1 + \varphi_2, \quad (12)$$

$$\varphi = (\varphi_1 - \varphi_2)/2, \quad (13)$$

$$\gamma(\phi) = \arctan(a \tan \phi/2), \quad (14)$$

and the asymmetry parameter

$$a = (E_{J1} - E_{J2})/(E_{J1} + E_{J2}). \quad (15)$$

Then the ratio of the critical currents of individual junctions is

$$r = I_{c2}/I_{c1} = E_{J2}/E_{J1} = (1 - a)/(1 + a). \quad (16)$$

We assume that $r \leq 1$, or, equivalently, $a \geq 0$, for definiteness.

A. Hamiltonian

In the case of a low impedance inserted into the Josephson circuit, for example, by means of a large shunting capacitance C_s ($e^2/2C_s \ll E_{J1,J2}$), associated, for example, with an additional parallel large Josephson junction [39], or a small shunting superconducting inductance [38, 40], or a small resistance [25], as in our case Eq. (2), phase ϕ is classical. (The BT characteristics in the opposite case of a high external impedance were reported in Refs. [43–45].) Then capacitances of individual Josephson junctions $C_{1,2}$ sum up with stray capacitance C_{stray} and give total capacitance of the island

$C_\Sigma = C_1 + C_2 + C_{\text{stray}}$. As a result, the charging energy of BT is equal to

$$E_c = e^2/2C_\Sigma. \quad (17)$$

The semi-difference phase φ Eq. (13) is associated with the island and in the case of non-vanishing E_c , phase φ behaves quantum mechanically. It is conjugate to the island charge $Q = -2ie\partial/\partial\varphi$ and obeys the commutation relation $[\varphi, Q] = 2ie$ [7].

The Hamiltonian of BT with fixed ϕ and zero gate current (i.e., the Cooper pair box configuration of BT [1, 46]) takes the form [23, 25]

$$H = \frac{Q^2}{2C_\Sigma} - E_J(\phi) \cos[\varphi + \gamma(\phi)], \quad (18)$$

yielding Schrödinger equation (in fact, the Mathieu equation):

$$\left[4E_c \frac{\partial^2}{\partial \chi^2} + E_J(\phi) \cos \chi - E \right] \psi = 0. \quad (19)$$

Here we introduced a new variable,

$$\chi = \varphi + \gamma(\phi), \quad (20)$$

by taking advantage of the relation $\partial/\partial\chi = \partial/\partial\varphi$. Then the individual junction phases are:

$$\varphi_1 = \chi - \gamma + \phi/2 \quad \text{and} \quad \varphi_2 = -\chi + \gamma + \phi/2. \quad (21)$$

Eigenvalue equation (19) yields the Bloch bands $E_n(q, \phi)$ with band index $n = 0, 1, 2, \dots$. These energies depend on quasicharge q (good variable) [8], while ϕ is real parameter [23]. For any n , even function $E_n(q, \phi)$,

$$E_n(-q, \phi) = E_n(q, \phi) \quad \text{and} \quad E_n(q, -\phi) = E_n(q, \phi), \quad (22)$$

obeys the double periodicity condition,

$$E_n(q, \phi) = E_n(q + 2e, \phi) = E_n(q, \phi + 2\pi). \quad (23)$$

The shape of the energy bands crucially depends on the characteristic energy ratio,

$$\lambda = (E_{J1} + E_{J2})/2E_c, \quad (24)$$

and the asymmetry parameter a Eq.(15). As an illustration, a 3D plot of the energy surfaces for the zeroth and the first Bloch bands is shown on Fig.2. Quantitatively, the shapes of the Bloch bands can be described by infinite matrices $\mathbf{A}^{(n)}$ with real elements

$$A_{km}^{(n)} = -\frac{1}{\pi e E_c} \int_0^\pi \int_0^e E_n(q, \phi) \cos \frac{k\pi q}{e} \cos m\phi dq d\phi, \quad (25)$$

entering the corresponding double Fourier series as coefficients (see Appendix A).

The eigenstates given by equation (19) are the Bloch waves,

$$\psi_q^{(n,\phi)}(\chi) = w_q^{(n,\phi)}(\chi) e^{i\pi q \chi / e}, \quad (26)$$

where $w_q^{(n,\phi)}(\chi)$ are the wave amplitudes and quasicharge q is the appropriate "crystal momentum" [8].

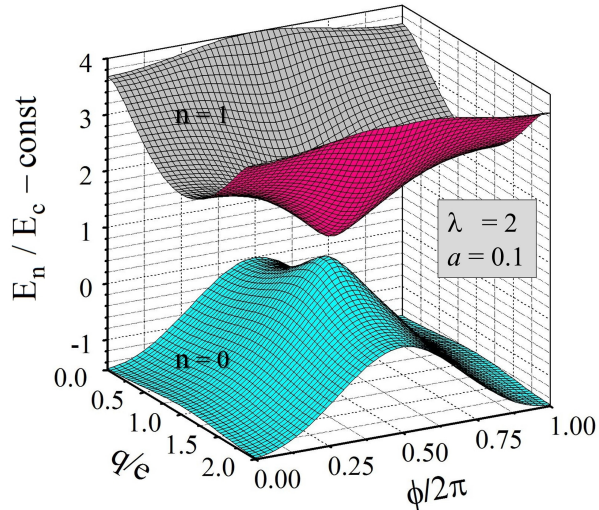


FIG. 2. Elementary cell ($0 \leq q \leq 2e$ and $0 \leq \phi \leq 2\pi$) of the double-periodic surfaces of the two lowest energy bands, i.e., the ground state band ($n = 0$) and the first band ($n = 1$). The specific shape of these Bloch bands has been used in engineering the charge-phase qubits with inherently small decoherence due to operating in the so-called sweet points [39, 41].

B. Voltage V_B and current I_s

In our analysis, we will focus on the ground state $E_0(q, \phi)$, assuming that the bath temperature T is low, i.e.,

$$k_B T \ll E_1(q, \phi) - E_0(q, \phi) \quad (27)$$

for all relevant q and ϕ . Moreover, we assume that the time-variations of quasicharge q and phase ϕ are sufficiently slow, so the system remains all the time in its instantaneous eigenstate given by bare Hamiltonian (18). Naturally, we exclude unwanted excitations of higher bands due to relatively fast motion. In the general case, phase operator χ has nonzero both intraband and interband components [47]. However, for fixed band index, $n = 0$, one can neglect the interband part of χ and consider that $[\chi, q] = 2ie$ [7, 8].

The electrical potential of the transistor island with respect to ground (see Fig. 1),

$$V_B = (\Phi_0/2\pi) \langle d\varphi_1/dt \rangle, \quad (28)$$

can be found using Eq.(21), i.e.,

$$\frac{2\pi}{\Phi_0} V_B = \langle \frac{d\varphi_1}{dt} \rangle = \langle \frac{\partial \chi}{\partial t} \rangle - \frac{\partial \gamma}{\partial \phi} \frac{\partial \phi}{\partial t} + \frac{1}{2} \frac{\partial \phi}{\partial t}, \quad (29)$$

where $\langle \dots \rangle$ denotes ensemble averaging. The first term is determined by the shape of the ground state energy [7, 8],

$$\frac{\Phi_0}{2\pi} \langle \frac{\partial \chi}{\partial t} \rangle = \frac{\partial E_0(q, \phi)}{\partial q} \equiv V_B^{(0)}(q, \phi). \quad (30)$$

This formula yields the island voltage $V_B^{(0)}$ at fixed ϕ (when both the second and the third terms in Eq.(29) are zero). Note, the island voltage derived (equivalently!) using phase φ_2 , i.e., $V_B = -(\Phi_0/2\pi) \langle \partial \varphi_2 / \partial t \rangle + V_J$, where voltage drop $V_J = (\Phi_0/2\pi) \partial \phi / \partial t$ (see Fig. 1), is given by the same formula Eq.(29).

Using explicit expression Eq.(14) for γ , the second and the third terms in Eq.(29) can be rewritten in the form:

$$-\frac{\partial \gamma}{\partial \phi} \frac{\partial \phi}{\partial t} + \frac{1}{2} \frac{\partial \phi}{\partial t} = -g(\phi) \frac{\partial \phi}{\partial t}, \quad (31)$$

where the periodic function $g(\phi)$,

$$g(\phi) = \frac{0.5a}{\cos^2(\phi/2) + a^2 \sin^2(\phi/2)} - 0.5, \quad (32)$$

has zero average value, i.e. $\int_0^{2\pi} g(\phi) d\phi = 0$. Summarizing, we obtain formula

$$V_B(q, \phi) = V_B^{(0)}(q, \phi) - \frac{\Phi_0}{2\pi} g(\phi) \frac{\partial \phi}{\partial t}, \quad (33)$$

where the second, dynamical term ($\propto d\phi/dt \neq 0$) is vanishingly small, for example, in the trivial case of a highly asymmetric BT, i.e., $r \rightarrow 0$ (or $a \rightarrow 1$).

Function $V_B^{(0)}(q, \phi)$ Eq.(30) is also double periodic,

$$V_B^{(0)}(q, \phi) = V_B^{(0)}(q + 2e, \phi) = V_B^{(0)}(q, \phi + 2\pi), \quad (34)$$

and odd (even) with respect to q (ϕ):

$$V_B^{(0)}(-q, \phi) = -V_B^{(0)}(q, \phi) \text{ and } V_B^{(0)}(q, -\phi) = V_B^{(0)}(q, \phi). \quad (35)$$

Its value is controlled by quasicharge q , determined by the injected current I_B [7],

$$q = q_0 + \int_0^t I_B(t') dt', \quad (36)$$

and apparently by phase ϕ .

Josephson supercurrent I_s flowing through BT also depends on these two variables. It can be expressed as an ensemble average of the time derivative of the corresponding charge operator $Q_s = -2ie\partial/\partial\phi$. This operator is conjugate to the phase operator ϕ . Thus,

$$I_s = \langle dQ_s/dt \rangle. \quad (37)$$

Using the Heisenberg equation of motion for operators, we obtain

$$I_s = -2ie \langle \frac{d}{dt} \frac{\partial}{\partial \phi} \rangle = \frac{2\pi}{\Phi_0} \langle [H, \frac{\partial}{\partial \phi}] \rangle = \frac{2\pi}{\Phi_0} \frac{\partial E_0(q, \phi)}{\partial \phi}. \quad (38)$$

Being a function of two classical variables, q and ϕ , supercurrent $I_s(q, \phi)$ is odd (even) function of ϕ (q), possessing double periodicity, i.e., [25],

$$I_s(q, -\phi) = -I_s(q, \phi) \text{ and } I_s(-q, \phi) = I_s(q, \phi), \quad (39)$$

$$I_s(q, \phi) = I_s(q, \phi + 2\pi) = I_s(q + 2e, \phi). \quad (40)$$

The current-phase relation, I_s versus ϕ , is non-sinusoidal for any q [25] (see Eq.(A6) in Appendix A) and the critical current value,

$$I_c(q) = \max_{\phi \in [0, \pi]} I_s(q, \phi), \quad (41)$$

is always smaller than the value in the double Josephson junction in the absence of the Coulomb blockade effect on the island ($E_c \rightarrow 0$) [23, 25, 48]. The periodic dependence of critical current I_c on quasicharge q was reported earlier, for example, in Refs.[49, 50]. In these experiments, q was fixed by a voltage applied to the capacitively coupled gate.

The expressions for functions $E_0(q, \phi)$, $V_B^{(0)}(q, \phi)$, and $I_s(q, \phi)$ in the form of the double Fourier series are given in Appendix A.

IV. EQUATIONS OF MOTION

We rewrite equations (4) and (5) in the dimensionless form using the normalizing units

$$V_u = (\pi/2)e/C_\Sigma \quad \text{and} \quad I_u = V_u/R_Q \quad (42)$$

for the voltage and the current, respectively. The dimensionless quasicharge is defined as

$$\theta = \pi q/e, \quad (43)$$

and the time derivatives are now denoted by a dot over the variables. Due to the periodic terms v_B and i_c , the oscillator equations for the Bloch and Josephson circuits,

$$\omega_{Bp}^{-2} \ddot{\theta} + \omega_{Bc}^{-1} \dot{\theta} + v_B(\theta, \phi) = v_0 + v_f, \quad (44)$$

$$\omega_{Jp}^{-2} \ddot{\phi} + \omega_{Jc}^{-1} \dot{\phi} + i_s(\theta, \phi) = i_0 + i_f, \quad (45)$$

mimic the RSJ model equations [33, 34]. Here the dimensionless BT voltage Eq.(33) includes two terms,

$$v_B(\theta, \phi) = v_B^{(0)}(\theta, \phi) - \omega_{Bc}^{-1} \alpha_B g(\phi) \dot{\phi}. \quad (46)$$

The corresponding "plasma" and "characteristic" frequencies in the Bloch and Josephson equations are defined as

$$\omega_{Bp} = \frac{\pi}{\sqrt{2L_b C_\Sigma}}, \quad \omega_{Bc} = \alpha_B \left(\frac{2\pi}{\Phi_0} \right) V_u, \quad (47)$$

and

$$\omega_{Jp} = \frac{\pi}{2R_Q \sqrt{C_\Sigma C_s}}, \quad \omega_{Jc} = \alpha_J \left(\frac{2\pi}{\Phi_0} \right) V_u, \quad (48)$$

respectively.

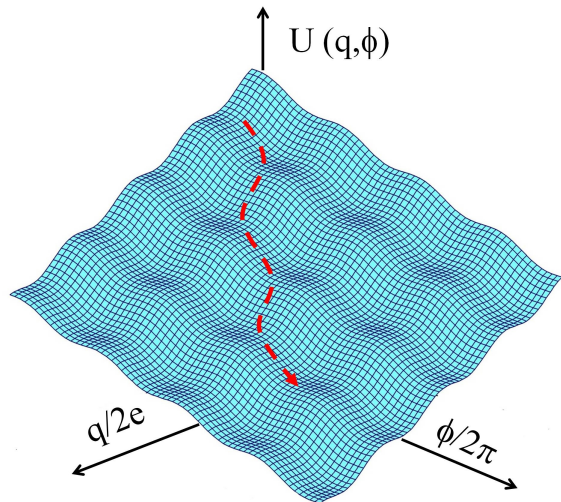


FIG. 3. Egg box potential Eq.(51) with adjusted individual slopes for variables θ and ϕ , ensuring steady motion downwards along "diagonal" path (schematically shown by the red dashed line). This motion is associated with the circuit operation, when a working point is fixed on the step. The dimensions of the egg-box elementary cell are 1×1 .

A. Egg box potential

The double periodic functions $v_B^{(0)}(\theta, \phi)$ and $i_s(\theta, \phi)$ in combination with voltage v_0 and current i_0 , included in the right hand sides of Eqs.(44)-(45), can be expressed via the derivatives of the dimensionless potential energy $u(\theta, \phi, v_0, i_0)$. Specifically,

$$v_B^{(0)}(\theta, \phi) - v_0 = \partial u / \partial \theta, \quad (49)$$

$$i_s(\theta, \phi) - i_0 = \partial u / \partial \phi, \quad (50)$$

where

$$u = U(\theta, \phi, v_0, i_0)/E_c = \varepsilon(\theta, \phi) - \theta v_0 - \phi i_0 \quad (51)$$

and $\varepsilon(\theta, \phi) = E_0(q, \phi)/E_c$ is the normalized ground state energy. Potential energy $U(\theta, \phi)$ Eq.(51) is two-dimensional analog of the well-known washboard potential playing pivotal role in physics of Josephson junctions [32]. In our case, the cosine Josephson potential is replaced by two-dimensional surface $\varepsilon(\theta, \phi)$ with double-periodic extrema and saddles. The shape of this surface mimics the shape of an egg box. Voltage v_0 and current i_0 are associated with the slopes for variables q and ϕ , respectively.

Figure 3 shows the egg box potential with sufficiently large slope (both v_0 and i_0 are above corresponding thresholds) to keep running states for both variables. It is intuitively clear, that for certain relation between v_0 and i_0 the synchronous motion of the two variables is possible along the "diagonal" path, schematically shown

by the red dashed line. Some tolerance of this running state to small variations of v_0 (or i_0) can be interpreted as a finite phase-locking range.

B. Operating Frequency

Let us make a comment concerning the operating frequency of the circuit, $\omega \sim \omega_B \sim \omega_J$, that is controlled by v_0 and i_0 entering into the right hand sides of Eqs. (44) and (45), respectively. Taking into account relation (3), we conclude that frequency $\omega_{Jc} \ll \omega_{Bc}$. We will assume that operating frequency $\omega \gg \omega_{Jc}$ and this inequality allows us to simplify solving the system of equations (44) and (45). Specifically, the nonlinear term $i_s(\theta, \phi)$ in Eq. (45) is much smaller than the second (dominant) term, $\omega_{Jc}^{-1} \dot{\phi} \sim \omega/\omega_{Jc} \gg 1$, hence, i_s can be considered as a small perturbation. Thus, backaction of the Bloch circuit on the Josephson circuit is negligibly small.

Note, that in the physical phenomenon of phase locking of two interacting generators, the regime when one device dominates the other is quite possible [51]. In our case, the slave Bloch oscillator is driven by the steady Josephson oscillator and this choice seems to be quite natural. Using the island capacitance $C_\Sigma \sim 1$ fF and taking the resistance value $R_s \sim 1 \Omega$, we arrive at the Josephson characteristic frequency of $\omega_{Jc}/2\pi \sim 20$ MHz. As will be shown below (see Eq. (81)), the differential resistance of the Bloch circuit at such low frequencies is rather high and the effect of noise is large. Thus, the beautiful case of truly mutual interaction of the Bloch and Josephson oscillators, occurring at low operating frequency, $\omega \sim \omega_{Jc}$, is seemingly of pure academic interest.

V. PHASE LOCKING

As long as the operating frequency $\omega \gg \omega_{Jc} \sim (2\pi/\Phi_0)R_s I_c(q)$, the Josephson circuit dynamics (45) is described by the RSJ model in the high-frequency limit [32]:

$$\dot{\phi} = \omega t + \tilde{\phi} + \phi_0 + \phi_f, \quad \omega = \omega_J = \frac{2\pi}{\Phi_0} \overline{V}_J \approx \frac{2\pi}{\Phi_0} I_0 R_s, \quad (52)$$

where we can neglect the small oscillating term $\tilde{\phi}$ and fix initial phase $\phi_0 = 0$. Noise variable ϕ_f obeys the stochastic equation,

$$\omega_{Jp}^{-2} \dot{\phi}_f + \omega_{Jc}^{-1} \dot{\phi}_f = i_f, \quad (53)$$

with Johnson noise term i_f on the right hand side. When $\omega_{Jp} \gg \omega_{Jc}$, i.e., in the case of relatively small capacitance C_s ($\beta_c \ll 1$), Eq. (53) is reduced to equation

$$\dot{\phi}_f = \omega_{Jc} i_f, \quad (54)$$

describing Brownian motion of phase ϕ_f , having a variance that increases linearly with time [52]. Substituting

relation Eq. (52) into Eq. (44) yields the equation solely for variable θ :

$$\begin{aligned} \omega_{Bp}^{-2} \ddot{\theta} + \omega_{Bc}^{-1} \dot{\theta} + v_B^{(0)}(\theta, \omega t + \phi_f) \\ = \omega \omega_{Bc}^{-1} \alpha_B g(\omega t + \phi_f) + v_0 + v_f. \end{aligned} \quad (55)$$

A. Autonomous I-V curve

Let us make several assumptions simplifying solving equation (55):

(i) Assuming that $\omega_{Bp} \gg \omega_{Bc}$ (the case of relatively low inductance L_b), we omit the first term on the left hand side of Eq. (55).

(ii) In both sums in the Fourier series representation of $v_B^{(0)}$ (A5), we keep only the first (dominant) terms, i.e.,

$$v_B^{(0)}(\theta, \phi) = u_c \sin \theta (1 + \mu \cos \phi), \quad (56)$$

where $u_c = 0.5 A_{10} = V_c/V_u$, $V_c = 0.25\pi A_{10} e/C_\Sigma$, and $\mu = 2|A_{11}|/A_{10}$.

(iii) Function $g(\omega t)$ contains the main tone ω and its harmonics $2\omega, 3\omega, \dots$ (see the shape of function g in Eq. (32)). The component oscillating with frequency ω is

$$[g(\phi)]_\omega = r \cos \phi, \quad (57)$$

where r is defined by Eq. (16). In fact, this term plays the role of small ac drive in equation Eq. (55). As long as small coefficient $\alpha_B \ll \omega/\omega_{Bc} \sim 1$, we can neglect that term.

Then the simplified equation of motion reads

$$\omega_{Bc}^{-1} \dot{\theta} + u_c \sin \theta [1 + \mu \cos(\omega t + \phi_f)] = v_0 + v_f. \quad (58)$$

This equation is similar to the RSJ model equation describing an effective Josephson junction with a modulated critical current. In the absence of modulation, $\mu = 0$, and noise, $v_f = 0$, it takes the form

$$\omega_c^{-1} \dot{\theta} + \sin \theta = \nu, \quad (59)$$

where

$$\omega_c = \omega_{Bc} u_c = \pi V_c / e R_b \quad \text{and} \quad \nu = v_0 / u_c. \quad (60)$$

The solution of this equation reads [32]:

$$\theta = 2 \arctan \left(\frac{\bar{i}}{\nu + 1} \tan \frac{\Theta}{2} \right) - \pi/2, \quad (61)$$

$$\dot{\theta} = \bar{i}^2 / (\nu - \sin \Theta), \quad (62)$$

$$\bar{i} = (\nu^2 - 1)^{1/2}, \quad (63)$$

$$\dot{\Theta} = \omega_c \bar{i}(\nu), \quad (64)$$

where Θ is the phase leader related to instant frequency of oscillations determined by

$$\bar{i} = \pi \bar{I} / e \omega_c = \omega_B / \omega_c. \quad (65)$$

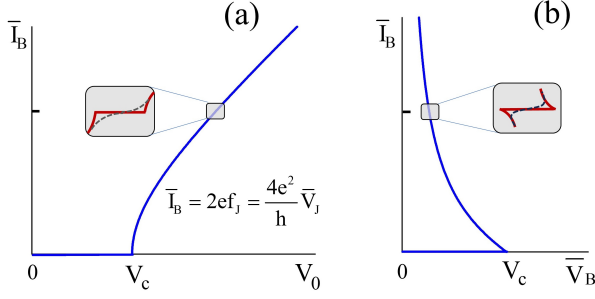


FIG. 4. Autonomous IV-curves of the Bloch circuit (the blue lines). The insets show the dual Shapiro steps of constant current in "embryo stage" ($\mu \rightarrow 1$), appearing at $\bar{I}_B = e\omega_J/\pi$. The dashed lines show the effect of relatively large noise. (a) Average current \bar{I}_B versus voltage V_0 . (b) The same I-V characteristic re-plotted as \bar{I}_B against \bar{V}_B .

Expression (63) gives the autonomous IV-curve,

$$\bar{I}_B = (V_0^2 - V_c^2)^{1/2}/R_b, \quad (66)$$

having standard hyperbolic shape, as shown in Fig. 4a. This curve is re-plotted in Fig. 4b as \bar{I}_B against $\bar{V}_B = V_0 - R_b \bar{I}_B$.

B. Formation of dual Shapiro step

In Josephson physics, Eq. (58) describes dynamics of a Josephson junction with an ac modulated critical current. This problem has been solved by Vanneste *et al.* in Ref. [53], where they had shown that the I-V curve exhibited the steps resembling the conventional Shapiro steps. Later on, such steps have been observed in the I-V curves of dc SQUID, modulated by an alternating magnetic flux [54], and in recent experiment [22], as dual Shapiro steps, when *microwave drive* was applied to the BT island. Below we show that these steps can appear on the I-V curve of BT due to modulation of its parameters by the oscillating Josephson supercurrent.

Under the assumption that parameter μ and the noise terms are small, we will consider them as small perturbation. In the vicinity of the expected step, the solution of equation (58) can be presented in the form:

$$\theta(t) = \theta_0(t) + \vartheta(t), \quad (67)$$

where phase $\vartheta(t)$ is a slow variable, i.e., $|\dot{\vartheta}| \ll \omega$. We will solve Eq. (58) using the slowly-varying phase method [55], adopted by Likharev (see Chapter 10 in Ref. [32]) for an ac driven Josephson junction.

We expand the needed solution $\theta(t)$ into the Taylor series

$$\theta = \theta_0 + \vartheta_1 + \vartheta_2 + \dots, \quad \vartheta_k \propto \epsilon^k, \quad k \geq 1, \quad (68)$$

with respect to small $\epsilon \propto \mu, \phi_f, v_f$. Then corresponding "correction" to dc voltage is

$$v_0 = \widehat{v}_0 + \widehat{v}_1 + \widehat{v}_2 + \dots, \quad \widehat{v}_k \propto \epsilon^k, \quad (69)$$

where $\widehat{(\dots)}$ denotes "intermediate" averaging over time interval Δt ,

$$\omega^{-1} \ll \Delta t \ll |\Omega|^{-1}, \quad (70)$$

where $\Omega = \omega_B - \omega$ is the small detuning (beating) frequency. Substitution of Eqs. (68) and (69) into Eq. (58) yields the system of the first three equations:

$$\omega_{Bc}^{-1} \dot{\theta}_0 + u_c \sin \theta_0 = \widehat{v}_0, \quad (71)$$

$$\begin{aligned} \omega_{Bc}^{-1} \dot{\vartheta}_1 + u_c \cos \theta_0 \vartheta_1 \\ = -\mu u_c \sin \theta_0 \cos(\omega t + \phi_f) + \widehat{v}_1 + v_f, \end{aligned} \quad (72)$$

$$\omega_{Bc}^{-1} \dot{\vartheta}_2 + u_c \cos \theta_0 \vartheta_2 = \widehat{v}_2 - 0.5 \sin \theta_0 \vartheta_1^2. \quad (73)$$

The solution of the first equation gives unperturbed I-V characteristic Eq. (66) and frequency of autonomous oscillations

$$\omega_A = \pi I_A/e = \pi(V_0^2 - V_c^2)^{1/2}/eR_b. \quad (74)$$

Following the approach developed in Ref. [32], we find the voltage correction terms (69) using the requirement of zero drift of phase, occurring due to terms $\vartheta_1, \vartheta_2, \dots$, i.e., $\widehat{\dot{\vartheta}}_k = 0$. Specifically, for $k = 1$ we have (cf. with Eq. (10.37) in Ref. [32])

$$[(\widehat{v}_1 - v_\mu + v_f)(\widehat{v}_0 - \sin \Theta)]^\wedge = 0, \quad (75)$$

where Θ is the phase leader. Thus, we obtain the expression for \widehat{v}_1 :

$$\widehat{v}_1 = \frac{\mu u_c}{2} \sin(\Theta - \omega t - \phi_f) - \frac{(v_f \sin \Theta)^\wedge}{v_0}. \quad (76)$$

Substituting $\widehat{v}_0 + \widehat{v}_1$ (both are slow variables) into the definition of the phase leader Eq. (64) and making replacement $\nu \rightarrow \nu + (v_1/u_c)$, we arrive at the equation for Θ :

$$\omega_c^{-1} \dot{\Theta} = \bar{i}(\nu) + (d\bar{i}/d\nu)v_1/u_c = \bar{i}_A + r_d^{-1}v_1(\Theta)/u_c, \quad (77)$$

where $r_d^{-1} = \nu/\bar{i} = \sqrt{1+i^{-2}} \cong \sqrt{1+(\omega_c/\omega)^2}$ is the dimensionless differential conductance and $d\bar{I}_B/dV_0 = 1/r_d R_b$. Here we expanded $\bar{i}(\nu)$ into the Taylor series and left only the term $\propto (v_1/u_c)$. Thus, the explicit formula for Θ reads

$$\omega_c^{-1} \dot{\Theta} = \bar{i} + r_d^{-1} \left[\frac{\mu \sin(\Theta - \omega t - \phi_f)}{2} - \frac{(v_f \sin \Theta)^\wedge}{u_c v_0} \right]. \quad (78)$$

Introducing a new (slow) variable, viz., the difference of the phase leaders of the Bloch oscillations and of the

Josephson ac drive, $\Theta_r = \Theta - \omega t + \phi_f$, we obtain the equation for Θ_r :

$$\dot{\Theta}_r = (\omega_A - \omega) + 0.5r_d^{-1}\omega_c\mu \sin \Theta_r + \omega_{Jc}i_f - \omega_c(v_f \sin \omega t)^{\wedge}. \quad (79)$$

The first term on the right hand side is the difference between frequency of autonomous oscillations and the drive frequency ω . The second term ($\propto \sin \Theta_r$) ensures phase locking of these two tones and, hence, is responsible for the step formation. In the absence of noise, the shape of this step mimics the shape of the autonomous curve in the vicinity of the Coulomb blockade ($\dot{\theta} = 0, I_B = 0$).

The third term in Eq. (79) is related to the noise, originated from the Josephson circuit. This noise is transferred to the Bloch circuit due to random drift ϕ_f of the total Josephson phase ϕ (see Eqs. (52), (53), and (54)). The fourth term is the noise originated from the Bloch circuit itself and down-converted from the oscillation frequency ω in the same manner as the noise in an ac driven Josephson junction [32]. Assuming that the noise sources Eqs. (7) and (8) are thermal with similar temperature T for both resistances R_s and R_b ($S_{I,V} \propto k_B T$, i.e., Johnson noise) and, hence, are independent of frequency, we can compare the contributions of the third and the fourth terms:

$$\frac{\langle \omega_{Jc}i_f \rangle_{\text{rms}}}{\langle \omega_c v_f \rangle_{\text{rms}}} = 0.5A_{10}(\alpha_J/\alpha_B)^{1/2} \ll 1. \quad (80)$$

Here we used Eqs. (48), (60), and (A7), and relation (3). Thus, we conclude that the Bloch circuit noise (the fourth term in Eq. (79)) dominates. Neglecting the third term makes equation Eq. (79) identical to that describing the effect of noise for the conventional Shapiro step (see Ref. [56] and Chapter 10 in Ref. [32]). The results of that study are obviously applicable to the case of a dual Shapiro step. The effective noise parameter is

$$\gamma_1 = 2\Gamma_1^{(A)}(eR_d/\pi\mu V_c), \quad (81)$$

where $2\Gamma_1^{(A)}$ is the linewidth of the autonomous Bloch oscillations. For sufficiently high frequency, $\omega \gg \omega_c$, the expression for the linewidth has a simple form, $2\Gamma_1^{(A)} = 2\pi(\pi/e)^2 k_B T/R_b$ (cf. with Eq. (4.37) in Ref. [32]). The effect of relatively large noise, $\gamma_1 \lesssim 1$, on the shape of the step is schematically shown in the insets in Fig. 4 by the dashed lines (cf. with Fig. 10.5 in Ref. [32]).

C. Size of the step

In essence, the obtained equation for the phase-leader difference Θ_r Eq. (79) is the RSJ model equation. Neglecting noise, this equation has a stationary solution, $\dot{\Theta}_r = 0$, existing in the range of the autonomous oscillation frequency ω_A given by the inequality

$$-\frac{\mu\omega_c}{2r_d} \leq \omega_A - \omega \leq \frac{\mu\omega_c}{2r_d}. \quad (82)$$

The resulting frequency range of phase-locking, $\Delta\omega_A = \mu\omega_c/r_d$, can be expressed in terms of the corresponding voltage V_0 (see Fig. 4a):

$$\Delta V = r_d R_b (e/\pi) \Delta\omega_A = \mu \frac{e\omega_c R_b}{\pi} = \mu V_c. \quad (83)$$

Thus, the step size is a factor of μ smaller than the nominal blockade voltage V_c .

Interestingly, formula Eq. (83) is valid for arbitrary μ . Neglecting the noise, solving general equation of motion (55) directly on the step (where Bloch and Josephson frequencies are equal and have constant phase difference Θ_r) is rather simple. Averaging of both sides of this equation over the period of oscillations, $2\pi/\omega = 2\pi/\dot{\theta}$, yields a dc term, periodically dependent on phase difference Θ_r . Specifically, using the Fourier-series representation Eq. (A5) we have

$$\overline{v_B^{(0)}} = 0.5 \sum_{k \geq 1} k A_{kk} \sin(k\Theta_r) \equiv F(\Theta_r). \quad (84)$$

Thus, the step size,

$$\Delta V = \frac{\pi e}{2C_\Sigma} \left[\max_{(0,\pi)} F(\Theta_r) - \min_{(-\pi,0)} F(\Theta_r) \right], \quad (85)$$

scales as C_Σ^{-1} and depends on the BT parameters λ and a .

Taking into account the dominant (first) term in the infinite series Eq. (84), we arrive at the following relation:

$$\Delta V \approx \frac{\pi e A_{11}}{4C_\Sigma} [\sin(-\pi/2) - \sin(\pi/2)] = \frac{\pi e}{2C_\Sigma} |A_{11}|, \quad (86)$$

or, using expression (A7) for blockade voltage V_c ,

$$\Delta V/V_c \approx 2|A_{11}|/A_{10} = \mu. \quad (87)$$

For example, for $\lambda = 0.5$ and $a = 0.1$, coefficients $A_{10} \approx 0.505$ and $A_{11} \approx -0.0979$ (see Eq. (A4)) give the relative step-size of $\Delta V/V_c \approx 0.39$. Taking into account the first three terms in Eq. (84) gives the value of $\Delta V/V_c \approx 0.42$.

D. Transconductance

When voltage V_0 is fixed such that average current $\overline{I_A}$ and, hence, ω_A correspond to the step center, the synchronization range Eq. (82) can be interpreted as the range of the Josephson frequency $\omega = \omega_J$, i.e.,

$$\omega_A - \mu\omega_c/2r_d \leq \omega \leq \omega_A + \mu\omega_c/2r_d. \quad (88)$$

Within this range the Bloch frequency, $\omega_B = \dot{\Theta} = \pi \overline{I_B}/e$, is phase-locked by the Josephson frequency, $\omega = (2\pi/\Phi_0)\overline{V_J}$, i.e., $\omega_B = \omega$. So, within the range Eq. (88) the BT transconductance is expressed via the fundamental constant, $\overline{I_B}/\overline{V_J} = R_Q^{-1}$.

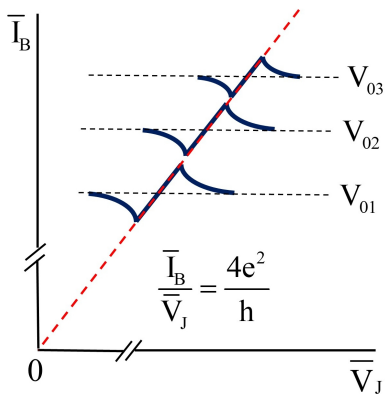


FIG. 5. Transconductance I-V curves exhibiting slanted steps, where both the differential transconductance $d\bar{I}_B/d\bar{V}_J$ and the ratio \bar{I}_B/\bar{V}_J take the fundamental value of R_Q^{-1} . The curves are plotted at sweep of current I_0 for three fixed values of voltage $V_0 = V_{01}, V_{02},$ and V_{03} .

The phase locking range can be expressed in terms of voltage \bar{V}_J as

$$\Delta\bar{V}_J = \frac{\Phi_0}{2\pi} \mu \omega_c / r_d = \mu \alpha_B V_c / r_d, \quad (89)$$

or, in terms of current \bar{I}_B ,

$$\Delta\bar{I}_B = \Delta\bar{V}_J / R_Q = \mu V_c / R_d, \quad (90)$$

where the differential resistance is given by the RSJ model, $R_d = r_d R_b = R_b / \sqrt{1 + (V_c / R_b \bar{I}_B)^2}$.

In the transconductance I-V characteristic, \bar{I}_B versus \bar{V}_J , the phase locking regime manifests itself as a slanted step with the fundamental slope of R_Q^{-1} . A series of such steps corresponding to different values of voltage V_0 is shown in Fig. 5. The red dashed line shows in this plot the locus of points corresponding to synchronous steady motion of quasicharge q and phase ϕ , although with a velocity depending on the working point on this line. This behavior has a clear interpretation using the egg box potential (see Fig. 3), where synchronous motion along the diagonal is obviously possible at different tilt angles of the ground energy band.

VI. DISCUSSION

We have described the mechanism of phase locking of the Bloch and Josephson oscillations assuming sufficiently high impedance of the Bloch circuit, i.e., $\alpha_B = R_Q / R_b \ll 1$. This condition is crucially important not only for our analysis Eq. (1), but also for the experimental observation of sufficiently sharp steps. The reason is noise associated with the quantum uncertainty of quasicharge because of appreciable coupling to environment.

Analysis of the case of not very small α_B has been performed in Refs. [57] and [58]. The obtained dual Shapiro steps have exhibited imperfect, smooth shapes. Specifically, the accuracy of the step position was poor (see Fig. 2 in Ref. [57]) and differential resistance on the step was at best of the order of hundreds k Ω [58]. Thus, the strategy in designing the experiment should include manufacturing sufficiently high resistance R_b . Moreover, its parasitic capacitance should contribute as small as possible value to the total capacitance of the island, C_Σ [59]. Then the values of the charging energy E_c , blockade voltage V_c , and, hence, step size ΔV are not notably diminished.

The step size ΔV Eq. (86) plays a critical role in the experiment, when noise is substantial. This can be, for example, because of Joule heating of the bias resistance R_b , leading to the increase of its effective electron temperature, $T^* > T$ [60]. Large ΔV forms large energy barrier $\Delta U = e\Delta V / 2\pi$ preventing diffusion of phase Θ_r and thereby ensures the flatness of the step. For thermal (markovian) noise, this process is described by corresponding Fokker-Plank equation [56].

In the experiments with external microwave drive, the size of a conventional Shapiro step (or a dual Shapiro step) is optimized by adjusting frequency and amplitude of the drive. Although the amplitude of modulation μ cannot be controlled in our circuit in the same way as in experiment with external ac signal, the obtained value of $\Delta V / V_c \approx 0.4$ is not small. It is comparable with the size of the first Shapiro step obtained in the RSJ model for an optimal amplitude of ac drive [61] (see also Fig. 11.4 in Ref. [32]). Interestingly, for achieving an appreciable size of the step, the microwave frequency should be about ω_c that corresponds to a relatively large dc current on the dual Shapiro step. Such current causes notable dissipation in the circuit and elevated electron temperature T^* . The dc driven Bloch circuit can operate at somewhat lower frequency (and, hence, lower current) without degradation of the step size. Moreover, in our case, the step size can be further optimized by adjusting the BT parameters. This can be done, for example, using the BT design shown in Fig. 6. Embedding a small

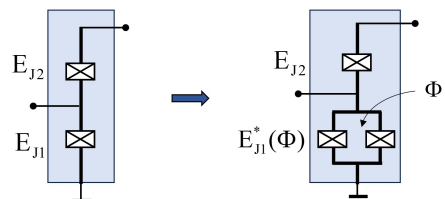


FIG. 6. Possible modification of BT enabling control of its asymmetry, $r = E_{J2} / E_{J1}^*(\Phi)$, and the ratio of characteristic energies λ Eq. 24. This control is done by applying external magnetic flux Φ to the dc SQUID loop encompassing two nearly equal small Josephson junctions.

dc SQUID instead of a single Josephson junction in one arm of the BT enables the control of the BT symmetry, $r = E_{J2}/E_{J1}^*(\Phi)$, and, partially, the control of the effective ratio of characteristic energies λ . The values of matrix elements Eq.(A4) in this BT can be tuned by external magnetic flux Φ . As a result, a somewhat larger value of coefficient A_{11} in Eq.(86) can be achieved.

Furthermore, the absence of external microwave signal may mitigate the effect of non-equilibrium noise in our the system. In particular, unwanted quasiparticle tunneling in the BT junctions, background charge noise in the substrate, and detrimental ac interferences on the chip which is shone by microwaves are presumably smaller in the *quiet*, i.e., without microwave drive, circuit shown in Fig.1. Thus, the observation of dual Shapiro steps in experiment with the BT driven only by dc sources seems to be quite feasible.

The obtained dual Shapiro steps are presumably horizontal, i.e., having strictly constant current position. The latter property is based on the assumption, that Josephson frequency ω_J is fixed Eq.(52) and, hence, independent of the working point on the step. In fact, a change of the working point on the step causes a small shift of the working point in the Josephson circuit and, as a consequence, a change of ω_J . In other words, it is a back-action of the Bloch circuit on the Josephson circuit, that was not taken into account in our model. However, it is easy to show that in the case of sufficiently low shunting resistance R_s Eq.(3), this effect is small and calculable. Specifically, the differential resistance on the dual Shapiro step is equal to R_Q^2/R_s . (This simple formula is derived in Appendix B.) For example, taking a rather conservative value of $R_s = 1 \Omega$, we obtain differential resistance $R_d^{(\text{step})}$ larger than 40 M Ω . Large value of $R_d^{(\text{step})}$ allows considering the effect of dual Shapiro steps in dc driven BT as a basis for application in metrology. Moreover, the facts that, firstly, the step center gives exact value of current, $\bar{I}_B = 2ef_J$, and, secondly, very small step-slope is well known, can substantially weaken the effect of the circuit parameters. Note, that the slope of the transconductance step Fig. 5 is independent of the circuit parameters and, therefore, *fundamental*. This quantum phenomenon may complete the original quantum metrology triangle [8] making it based entirely on superconducting components, as shown in Fig. 7.

For the sake of brevity, we have been focused only on the fundamental dual Shapiro step, occurring at $\omega_B = \omega_J$. Of course, the BT properties allow coupling of harmonics of these frequencies, i.e., $k\omega_B = m\omega_J$. This conclusion follows from the premise, that nonzero matrix element A_{km} in Eq.(A4) naturally determines the size of the corresponding fractional step. On the other hand, the absolute values of such matrix elements are clearly smaller than $|A_{11}|$ and, consequently, the experimental observation of these fractional steps in the presence of appreciable noise is more challenging.

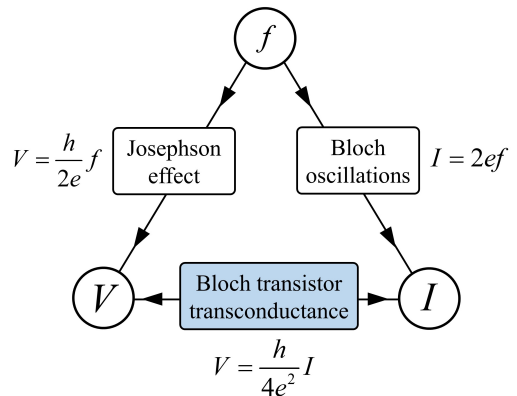


FIG. 7. *Superconducting* version of the quantum metrology triangle. Quantum Hall effect, based on 2D electron systems in high magnetic field (it was included in the original version of the triangle for linking V and I [8]) is replaced by superconducting BT ensuring the fundamental value of resistance for the bottom side of the triangle.

VII. CONCLUSION

In conclusion, we have proposed a circuit including BT and two independent electrical sources controlling its complementary variables, quasicharge q and phase ϕ . We have shown that the shape of the ground state energy in BT gives a unique possibility to mutually couple two different types of oscillations, viz., the Josephson oscillations and Bloch oscillations. There is a finite range of control parameters where these oscillations are phase locked. On the I-V curves of the Bloch circuit, this phase-locking range manifests itself as a dual Shapiro step. Realization of dual Shapiro steps using remarkable properties of BT fed by dc sources could be an interesting experiment per se. The state of the art technology and proficiency, accumulated in recent experiments, is a good basis for the fast progress in this experiment.

As long as the frequencies of Bloch and Josephson oscillations are linked to the constant voltage and constant current by means of the fundamental constants, Φ_0 and $2e$, respectively, the BT transconductance takes on the step the fundamental value of $2e/\Phi_0 = 4e^2/h$. The results of our study lead to the updated version of the quantum metrology triangle, based entirely on superconducting elements. The proposed circuit paves the way to the alternative quantum standard of resistance operating without strong magnetic field (cf. with the present 2DEG-based resistance standard [27]). After improvement of experiment, this triangle will certainly have great impact on possible refining the values of h and e , which are the basis for modern electrical metrology [62]. Comparison of "superconducting" and 2DEG-based quantum conductances with revising the value of fine structure constant could be another milestone goal.

We believe that our results will trigger further devel-

opment of the Bloch oscillation experiments based on advanced fabrication technology, modern cryogenic instrumentation and new ideas in designing superconducting quantum circuits.

ACKNOWLEDGMENTS

The author is grateful to Yuri Pashkin for stimulating discussions and useful comments.

Appendix A: Fourier series representation of $V_B(q, \phi)$ and $I_s(q, \phi)$

Due to double periodicity Eq.(23) and evenness Eq.(22) of the ground-state energy $E_0(q, \phi)$, it can be represented as a double Fourier series,

$$\begin{aligned} \varepsilon(\theta, \phi) = & -0.5 \sum_{k \geq 1} A_{k0} \cos(k\theta) - 0.5 \sum_{m \geq 1} A_{0m} \cos(m\phi) \\ & - \sum_{k, m \geq 1} A_{km} \cos(k\theta) \cos(m\phi) + 0.25A_{00}, \quad (\text{A1}) \end{aligned}$$

where the dimensionless energy and quasicharge are

$$\varepsilon = E_0(q, \phi)/E_c \quad \text{and} \quad \theta = \pi q/e. \quad (\text{A2})$$

The Fourier coefficients in Eq.(A1) are

$$A_{km} = -\frac{4}{\pi^2} \int_0^\pi \int_0^\pi \varepsilon(\theta, \phi) \cos(k\theta) \cos(m\phi) d\theta d\phi, \quad (\text{A3})$$

where integer numbers $k \geq 0$ and $m \geq 0$.

Elements A_{km} of infinite matrix \mathbf{A} depend on parameter λ Eq.(24) and the asymmetry factor a Eq.(15). For typical experimental values of BT parameters ($\lambda \sim 1$ and not extremely small a), the ground energy profile $E_0(q, \phi)$ is obviously smooth and the absolute values $|A_{km}|$ steeply decay with a rise of k or/and m . As an illustration, the most essential part of matrix \mathbf{A} , numerically calculated for $\lambda = 0.5$ and $a = 0.1$, is given below:

$$\mathbf{A} = \begin{bmatrix} & 0.6037 & -0.0386 & 0.0094 & \dots \\ \mathbf{0.5055} & \mathbf{-0.0979} & 0.0237 & -0.0064 & \dots \\ -0.0685 & 0.0317 & -0.0126 & 0.0051 & \dots \\ 0.0193 & -0.0112 & 0.0067 & -0.0034 & \dots \\ \dots & \dots & \dots & \dots & \dots \end{bmatrix}, \quad (\text{A4})$$

where unimportant matrix element A_{00} , associated with an additive constant, is omitted. The dominant matrix elements, A_{10} and A_{11} , giving approximate width of the dual Shapiro step Eq. (87) are marked by bold font.

For dimensionless voltage $v_B^{(0)} = V_B^{(0)}/V_u$ and current $i_s = I_s/I_u$, using Eqs.(30) and (38), we obtain the Fourier series:

$$\begin{aligned} v_B^{(0)}(\theta, \phi) = & 0.5 \sum_{k \geq 1} k A_{k0} \sin(k\theta) \\ & + \sum_{k, m \geq 1} k A_{km} \sin(k\theta) \cos(m\phi) \quad (\text{A5}) \end{aligned}$$

and

$$\begin{aligned} i_s(\theta, \phi) = & 0.5 \sum_{m \geq 1} m A_{0m} \sin(m\phi) \\ & + \sum_{k, m \geq 1} m A_{km} \cos(k\theta) \sin(m\phi), \quad (\text{A6}) \end{aligned}$$

respectively.

The first sum in Eq. (A5) (Eq. (A6)) is independent of variable ϕ (variable θ). So, this part of voltage (current) is decoupled from the complementary variable phase ϕ (quasicharge θ). The first terms in these series dominate and, hence, they give the estimates of the blockade voltage and the critical current of BT, respectively. Specifically, voltage

$$V_c \approx \frac{\pi e}{4C_\Sigma} A_{10}; \quad (\text{A7})$$

similarly, the critical current is

$$I_c \sim \frac{\pi e}{4R_Q C_\Sigma} A_{01}. \quad (\text{A8})$$

Because the current-phase relation in BT is inherently non-sinusoidal [25], the latter relation, containing only one term from the double series (A6), is a rough estimate.

Appendix B: Slope of dual Shapiro step

To find the correction to Josephson frequency ω_J , we take into account relatively small term i_s in Eq. (45). On the step, the slowly varying part of current i_s is given by formula (A6),

$$\hat{i}_s = -0.5 \sum_{m \geq 1} m A_{mm} \sin(m\Theta_r) \approx -0.5 A_{11} \sin \Theta_r. \quad (\text{B1})$$

As a result, the constant current term i_0 in Eq. (45) takes the form,

$$i_0 \rightarrow i_0 + \Delta i_0, \quad \text{where} \quad \Delta i_0 = 0.5 A_{11} \sin \Theta_r. \quad (\text{B2})$$

The corresponding correction to dc voltage \bar{V}_J is

$$\Delta \bar{V}_J = \Delta i_0 I_u R_d^{(J)} \approx \alpha_J \frac{\pi e}{2C_\Sigma} \Delta i_0, \quad (\text{B3})$$

where we used the fact, that differential resistance in the Josephson circuit is $R_d^{(J)} \approx R_s$.

On the step, the Josephson and Bloch frequencies are equal and the difference of their phases Θ_r is fixed. Hence, the above correction to \bar{V}_J is straightforwardly translated to corrections of \bar{I}_B , i.e.,

$$\Delta \bar{I}_B(\Theta_r) = R_Q^{-1} \Delta \bar{V}_J(\Theta_r). \quad (\text{B4})$$

Thus, the total change of current \bar{I}_B for scanning from one edge of the step ($\Theta_r = -\pi/2$) to the other ($\Theta_r = \pi/2$) is

$$\delta \bar{I}_B = \Delta \bar{I}_B(-\pi/2) - \Delta \bar{I}_B(\pi/2) = \frac{\pi e \alpha_J}{2R_Q C_\Sigma} |A_{11}|. \quad (\text{B5})$$

Comparison of Eq. (B5) with formula (86) for the dual Shapiro step size, yields the differential resistance on the

step, i.e.,

$$R_d^{(\text{step})} = \Delta V / \delta \bar{I}_B = R_Q / \alpha_J = R_Q^2 / R_s. \quad (\text{B6})$$

-
- [1] Y. A. Pashkin, O. Astafiev, T. Yamamoto, Y. Nakamura, and J. S. Tsai, Josephson charge qubits: a brief review, *Quantum Inf. Processing* **8**, 55 (2009).
- [2] J. Koch, T. M. Yu, J. Gambetta, A. A. Houck, D. I. Schuster, J. Majer, A. Blais, M. H. Devoret, S. M. Girvin, and R. J. Schoelkopf, Charge-insensitive qubit design derived from the Cooper pair box, *Phys. Rev. A* **76**, 042319 (2007).
- [3] J. Clarke and F. Wilhelm, Superconducting quantum bits, *Nature* **453**, 1031 (2008).
- [4] V. E. Manucharyan, J. Koch, L. I. Glazman, and M. H. Devoret, Fluxonium: Single Cooper-pair circuit free of charge offsets, *Science* **326**, 113 (2009).
- [5] Y. Makhlin, G. Schön, and A. Shnirman, Quantum-state engineering with Josephson-junction devices, *Rev. Mod. Phys.* **73**, 357 (2001).
- [6] I. V. Pechenezhskiy, R. A. Mencia, L. B. Nguyen, Y. H. Lin, and V. E. Manucharyan, The superconducting quasicarrier qubit, *Nature* **585**, 368 (2020).
- [7] D. V. Averin, A. B. Zorin, and K. K. Likharev, Bloch oscillations in small Josephson junctions, *Zh. Eksp. Teor. Fiz.* **88**, 692 (1985), [*Sov. Phys. JETP* **61**, 407-413 (1985)].
- [8] K. K. Likharev and A. B. Zorin, Theory of the Bloch-wave oscillations in small Josephson junctions, *J. Low Temp. Phys.* **59**, 347–382 (1985).
- [9] B. D. Josephson, Possible new effects in superconductive tunnelling, *Physics Letters* **1**, 251 (1962).
- [10] L. S. Kuzmin and D. B. Haviland, Observation of the Bloch oscillations in an ultrasmall Josephson junction, *Phys. Rev. Lett.* **67**, 2890 (1991).
- [11] L. S. Kuzmin and D. B. Haviland, Bloch oscillations and Coulomb blockade of Cooper pair tunneling in ultrasmall Josephson junctions, *Phys. Scripta* **1992**, 171 (1992).
- [12] L. S. Kuzmin, Y. A. Pashkin, and T. Claeson, Bloch oscillations in a double Josephson junction biased via high-ohmic resistors, *Supercond. Sci. Technol.* **7**, 324 (1994).
- [13] Y. A. Pashkin, C. D. Chen, D. B. Haviland, and L. S. Kuzmin, Magnetic field dependence of the current-voltage curve of a superconducting single electron transistor in a high impedance environment, *Czech. J. Phys.* **46**, 2291 (1996).
- [14] M. Watanabe and D. B. Haviland, Coulomb blockade and coherent single-Cooper-pair tunneling in single Josephson junctions, *Phys. Rev. Lett.* **86**, 5120 (2001).
- [15] S. V. Lotkhov, Ultra-high-ohmic microstripline resistors for Coulomb blockade devices, *Nanotechnology* **24**, 235201 (2013).
- [16] L. Grünhaupt, M. Spiecker, D. Gusenkova, N. Maleeva, S. T. Skacel, I. Takmakov, F. Valenti, P. Winkel, H. Rotzinger, W. Wernsdorfer, A. V. Ustinov, and I. M. Pop, Granular aluminium as a superconducting material for high-impedance quantum circuits, *Nat. Materials* **18**, 816 (2019).
- [17] F. Kaap, D. Scheer, F. Hassler, and S. Lotkhov, Synchronization of Bloch oscillations in a strongly coupled pair of small Josephson junctions: Evidence for a Shapiro-like current step, *Phys. Rev. Lett.* **132**, 027001 (2024).
- [18] F. Kaap, C. Kissling, V. Gaydamachenko, L. Grünhaupt, and S. Lotkhov, Demonstration of dual Shapiro steps in small Josephson junctions, *Nat. Commun.* **15**, 8726 (2024).
- [19] N. Crescini, S. Cailleaux, W. Guichard, C. Naud, O. Buisson, K. W. Murch, and N. Roch, Evidence of dual Shapiro steps in a Josephson junction array, *Nat. Phys.* **19**, 851 (2023).
- [20] R. S. Shaikhaidarov, K. H. Kim, J. Dunstan, I. Antonov, V. N. Antonov, and O. V. Astafiev, Quantized current steps due to the synchronization of microwaves with Bloch oscillations in small Josephson junctions, *Nat. Commun.* **15**, 9326 (2024).
- [21] R. S. Shaikhaidarov, K. H. Kim, J. W. Dunstan, I. V. Antonov, S. Linzen, M. Ziegler, D. S. Golubev, V. N. Antonov, E. V. Il'ichev, and O. V. Astafiev, Quantized current steps due to the a.c. coherent quantum phase-slip effect, *Nature* **608**, 45 (2022).
- [22] I. Antonov, R. S. Shaikhaidarov, K. H. Kim, D. Golubev, S. Linzen, E. V. Il'ichev, V. N. Antonov, and O. V. Astafiev, Demonstration of dual Shapiro steps in small Josephson junctions, *Nat. Commun.* **17**, 1264 (2026).
- [23] K. K. Likharev, Coexistence of Bloch and Josephson effects, and resistance quantization in small-area layered superconducting structures, M. V. Lomonosov Moscow State University, Department of Physics (1986), preprint No. 29/1986.
- [24] K. K. Likharev and A. B. Zorin, Simultaneous Bloch and Josephson oscillations, and resistance quantization in small superconducting double junctions, *Jpn. J. Appl. Phys.* **26**, 1407 (1987).
- [25] A. B. Zorin, Quantum-limited electrometer based on single Cooper pair tunneling, *Phys. Rev. Lett.* **76**, 4408 (1996).
- [26] K. v. Klitzing, G. Dorda, and M. Pepper, New method for high-accuracy determination of the fine-structure constant based on quantized Hall resistance, *Phys. Rev. Lett.* **45**, 494 (1980).
- [27] K. v. Klitzing, The quantized Hall effect, *Rev. Mod. Phys.* **58**, 519 (1986).
- [28] R.-P. Riwar, M. Houzet, J. S. Meyer, and Y. V. Nazarov, Multi-terminal Josephson junctions as topological matter, *Nat. Commun.* **7**, 11167 (2016).
- [29] E. Eriksson, R.-P. Riwar, M. Houzet, J. S. Meyer, and Y. V. Nazarov, Topological transconductance quantization in a four-terminal Josephson junction, *Phys. Rev. B* **95**, 075417 (2017).
- [30] A. M. Hriscu and V. V. Nazarov, Quantum synchronization of conjugated variables in a superconducting device leads to the fundamental resistance quantization, *Phys. Rev. Lett.* **110**, 097002 (2013).
- [31] R. S. Shaikhaidarov, I. Antonov, K. H. Kim, A. Shes-

- terikov, S. Linzen, E. V. Il'ichev, V. N. Antonov, and O. V. Astafiev, Feasibility of the Josephson voltage and current standards on a single chip, *Appl. Phys. Lett.* **125**, 122602 (2024).
- [32] K. K. Likharev, *Dynamics of Josephson junctions and circuits* (Gordon and Breach, New York, 1986).
- [33] D. E. McCumber, Effect of ac impedance on dc voltage-current characteristics of superconductor weak-link junctions, *J. Appl. Phys.* **39**, 3113 (1968).
- [34] W. C. Stewart, Current-voltage characteristics of Josephson junctions, *Appl. Phys. Lett.* **12**, 277 (1968).
- [35] J. Aumentado, M. W. Keller, J. M. Martinis, and M. H. Devoret, Nonequilibrium quasiparticles and $2e$ periodicity in single-Cooper-pair transistors, *Phys. Rev. Lett.* **92**, 066802 (2004).
- [36] H. Q. Nguyen, T. Aref, V. J. Kauppila, M. Meschke, C. B. Winkelmann, H. Courtois, and J. P. Pekola, Trapping hot quasi-particles in a high-power superconducting electronic cooler, *New Journal of Physics* **15**, 085013 (2013).
- [37] V. Iaia, J. Ku, A. Ballard, C. P. Larson, E. Yelton, C. H. Liu, S. Patel, R. McDermott, and B. L. T. Plourde, Phonon downconversion to suppress correlated errors in superconducting qubits, *Nat. Commun.* **13**, 6425 (2022).
- [38] A. B. Zorin, Radio-frequency Bloch-transistor electrometer, *Phys. Rev. Lett.* **86**, 3388 (2001).
- [39] D. Vion, A. Aassime, A. Cottet, P. Joyez, H. Pothier, C. Urbina, D. Esteve, and M. H. Devoret, Manipulating the quantum state of an electrical circuit, *Science* **296**, 886 (2002).
- [40] A. B. Zorin, Cooper-pair qubit and Cooper-pair electrometer in one device, *Physica C* **368**, 284 (2002).
- [41] A. B. Zorin, Josephson charge-phase qubit with the radio frequency readout: coupling and decoherence, *Zh. Eksp. Teor. Fiz.* **125**, 1423 (2004), [*JETP* **98**, 1250-1261 (2004)].
- [42] A. Barone and G. Paterno, *Physics and Applications of the Josephson Effect* (John Wiley & Sons Inc., New York, 1982).
- [43] A. B. Zorin, Y. A. Pashkin, V. A. Krupenin, and H. Scherer, Coulomb blockade electrometer based on single Cooper pair tunneling, *Appl. Supercond.* **6**, 453 (1998).
- [44] A. B. Zorin, S. V. Lotkhov, Y. A. Pashkin, H. Zangerle, V. A. Kruperin, T. Weimann, H. Scherer, and J. Niemeyer, Highly sensitive electrometers based on single Cooper pair tunneling, *J. Supercond.* **12**, 747 (1999).
- [45] M. Houzet, T. Vakhel, and J. S. Meyer, Bloch diode, *Phys. Rev. Lett.* **136**, 146001 (2026).
- [46] V. Bouchiat, D. Vion, P. Joyez, D. Esteve, and M. H. Devoret, Quantum coherence with a single Cooper pair, *Phys. Scripta* **1998**, 165 (1998).
- [47] E. M. Lifshitz and L. P. Pitaevskii, *Statistical Physics, Part 2: Theory of the Condensed State (Course of Theoretical Physics Vol. 9)* (Pergamon Press / Butterworth-Heinemann, 1980).
- [48] K. A. Matveev, M. Gisselält, L. I. Glazman, M. Jonson, and R. I. Shekhter, Parity-induced suppression of the Coulomb blockade of Josephson tunneling, *Phys. Rev. Lett.* **70**, 2940 (1993).
- [49] P. Joyez, P. Lafarge, A. Filipe, D. Esteve, and M. H. Devoret, Observation of parity-induced suppression of Josephson tunneling in the superconducting single electron transistor, *Phys. Rev. Lett.* **72**, 2458 (1994).
- [50] T. M. Eiles and J. M. Martinis, Combined Josephson and charging behavior of the supercurrent in the superconducting single-electron transistor, *Phys. Rev. B* **50**, 627 (1994).
- [51] V. V. Migulin, V. I. Medvedev, E. R. Mustel, and V. N. Parygin, *Basic Theory of Oscillations* (Mir, Moscow, 1983).
- [52] S. A. Akhmanov, Y. E. Djakov, and A. S. Chirkin, *Vvedeniye v statisticheskuyu radiofiziku i optiku (Introduction to Statistical Radiophysics and Optics)* (Nauka, Moscow, 1981) [In Russian].
- [53] C. Vanneste, A. Gilabert, P. Sibillot, and D. B. Ostrowsky, Josephson steps produced by critical current amplitude modulation, *J. Low Temp. Phys.* **45**, 517–530 (1981).
- [54] C. Vanneste, C. C. Chi, W. J. Gallagher, A. W. Kleinsasser, S. I. Raider, and R. L. Sandstrom, Shapiro steps on current-voltage curves of dc SQUIDS, *J. Appl. Phys.* **64**, 242 (1988).
- [55] N. N. Bogoliubov and Y. A. Mitropolski, *Asymptotic Methods in the Theory of Non-Linear Oscillations* (Gordon and Breach, New York, 1961).
- [56] M. J. Stephen, Noise in a driven Josephson oscillator, *Phys. Rev.* **186**, 393 (1969).
- [57] A. D. Marco, F. W. J. Hekking, and G. Rastelli, Quantum phase-slip junction under microwave irradiation, *Phys. Rev. B* **91**, 184512 (2015).
- [58] M. Resch, J. Ankerhold, B. I. C. Donvil, P. Muratore-Ginanneschi, and D. Golubev, Quantum and classical Shapiro steps in small Josephson junctions (2025), arXiv:2508.04574 [cond-mat.supr-con].
- [59] L. Arndt, A. Roy, and F. Hassler, Dual Shapiro steps of a phase-slip junction in the presence of a parasitic capacitance, *Phys. Rev. B* **98**, 014525 (2018).
- [60] F. Maibaum, S. V. Lotkhov, and A. B. Zorin, Towards the observation of phase-locked Bloch oscillations in arrays of small Josephson junctions, *Phys. Rev. B* **84**, 174514 (2011).
- [61] K. K. Likharev and V. K. Semenov, Electrodynamic properties of superconducting point contacts, *Radiotekhnika i elektronika* [in Russian] **16**, 2167 (1971), [*Radio Eng. Electron. Phys. (USSR)* (Engl. Transl.) **16**, 1917 (1971)].
- [62] D. S. Wiersma and G. Mana, The fundamental constants of physics and the international system of units, *Rend. Fis. Acc. Lincei* **32**, 655 (2021).